Electrochemistry
The Electrochemical Society of Japan
Received: November 16, 2011
Accepted: February 4, 2012
Published: May 5, 2012
http://dx.doi.org/10.5796/electrochemistry.80.318
JOI:JST.JSTAGE/electrochemistry/80.318
Communication
Electrochemistry, **80(5)**, 318–320 (2012)

An Oxygen Responsive Microparticle-Patterned Hydrogel Sheet for Enzyme Activity Imaging

Kuniaki NAGAMINE,[a,b] Shuntaro ITO,[a] Mai TAKEDA,[a] Shingo OTANI,[a] and Matsuhiko NISHIZAWA[a,b,*]

[a] *Department of Bioengineering and Robotics, Graduate School of Engineering, Tohoku University, 6-6-01 Aramaki, Aoba-ku, Sendai 980-8579, Japan*
[b] *JST-CREST, Sanbancho, Chiyoda-ku, Tokyo 102-0075, Japan*

* *Corresponding author: nishizawa@biomems.mech.tohoku.ac.jp*

ABSTRACT

A patch-type oxygen imaging sheet useful for in vitro cellular metabolic assays was developed. Oxygen-responsive fluorescent microbeads were embedded into a biocompatible polyacrylamide gel sheet, which can be directly attached onto target cells for fluorescent imaging of metabolic activity. The sensor beads were directed in a microfluidic device using AC and DC electric manipulation techniques, followed by encapsulation in a hydrogel. Fluorescent imaging of oxygen-consuming activity was demonstrated for glucose oxidase-modified microparticles as cellular models to show the applicability of the imaging sheet to bioassays.

Keywords : Electrohydrodynamics, Microfluidic Device, Oxygen Imaging Sheet

1. Introduction

In vitro bioassays of cellular metabolic activity have been carried out to investigate the cell physiology. Evaluation of the oxygen-consuming activity of cells is significant for the indirect investigation of glucose metabolic activity. Such oxygen sensing would be applicable for revealing the mechanism of controlling blood glucose homeostasis and pathogenesis of type 2 diabetes using an insulin-responsive skeletal muscle cell.

In recent years, 2D fluorescent imaging sheets have been actively developed for mapping metabolite distribution in tissues.[1–4] In particular, Wolfbeis et al.[2,3] showed the applicability of pH- and oxygen-responsive sheets in animal experiments. All previous work used sheets in which the sensor microparticles were uniformly dispersed. However, the metabolite diffusion area is confined to the immediate vicinity of the cells. Besides, uniformly dispersed particles modify the characteristics of the hydrogel such as flexibility and nutrient permeability,[5] which will affect muscle cellular contractility and metabolic activity. In this study, the sensor beads were localized on the surface of the imaging sheet using AC and DC electric manipulation techniques to increase the surface sensitivity without sacrificing the merits of original gel characteristics. Fluorescent imaging of oxygen-consuming activity was demonstrated for glucose oxidase (GOD)-modified particles as cellular models (Fig. 1). When GOD-catalyzed glucose oxidation consumes the oxygen, the fluorescent intensity of the sensor beads increases in a pattern representing GOD activity.

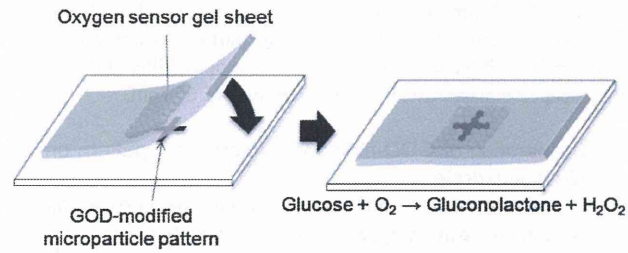

Figure 1. Schematic view of oxygen imaging around the pre-patterned GOD-modified microparticles.

2. Experimental

2.1 Preparation of oxygen responsive microparticles

A 3.5 mL of aqueous polystyrene microparticle suspension (1.0 μm diameter, Micromod) was mixed with 1.5 mL of tetrahydrofuran (THF) under ultrasonication for 10 min to swell the particles. A 0.5 mL solution of oxygen responsive fluorescent dye, platinum octaethylporphyrin (PtOEP, Sigma-Aldrich), dissolved in dimethyl sulfoxide was added to the particle suspension followed by another 20 min ultrasonication to incorporate the PtOEP into the particles.[6] Then, THF in the mixture was evaporated for 12 h at room temperature. The particles were separated by centrifugation, and washed two times with ethanol.

2.2 Fabrication of the microfluidic device

The microfluidic device was composed of three layers; an ITO top layer, a silicone rubber middle layer, and an ITO bottom layer covered with a negative photoresist SU-8 3005 pattern as an insulator. The silicone rubber layer had a stenciled opening that became the interior of the microchannel when sandwiched between the top and bottom ITO layers. The resulting microchannel was 10 mm in width and 500 μm in height. The channel inlet was connected to the particle suspension reservoir, and its outlet was attached to a syringe pump (World Precision Instruments) to introduce the particles into the channel.

2.3 Fabrication of the oxygen imaging sheet

The oxygen-responsive microparticles suspended in 0.5 mM NaCl solution were injected into the microchannel, and a sinusoidal AC voltage (100 Hz, 10 Vpp) was applied between the top and bottom ITO electrodes (Fig. 2A). The resulting AC electric field is strongest on the surface of the bottom ITO electrode, and the electrohydrodynamic force induces particle motion toward the bottom ITO pattern (1 mm × 1 mm). Then, the power supply was

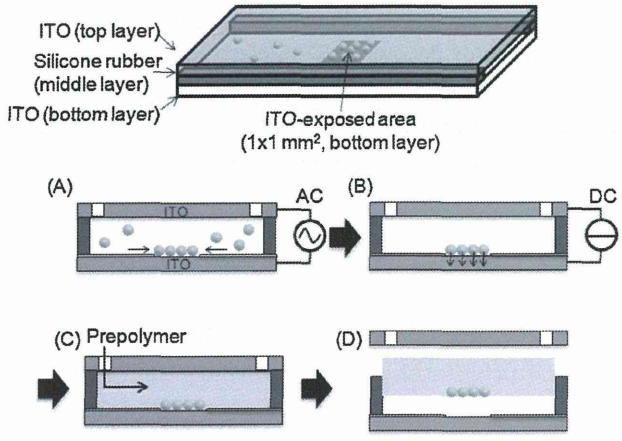

Figure 2. Preparation of the hydrogel sheet with patterned oxygen-responsive microparticles.

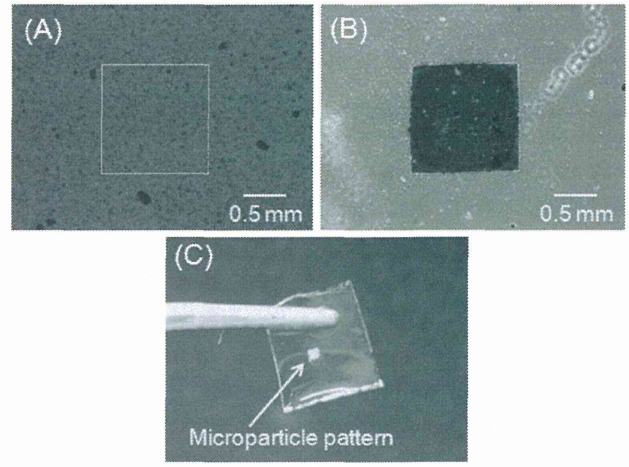

Figure 3. (A, B) Phase contrast micrographs (A) before and (B) after application of AC voltage between the top and bottom ITO electrodes. White-dashed line in (A) represents the ITO pattern on the bottom of the microchannel. (C) Photograph of the polyacrylamide hydrogel sheet with the oxygen responsive microparticle pattern embedded.

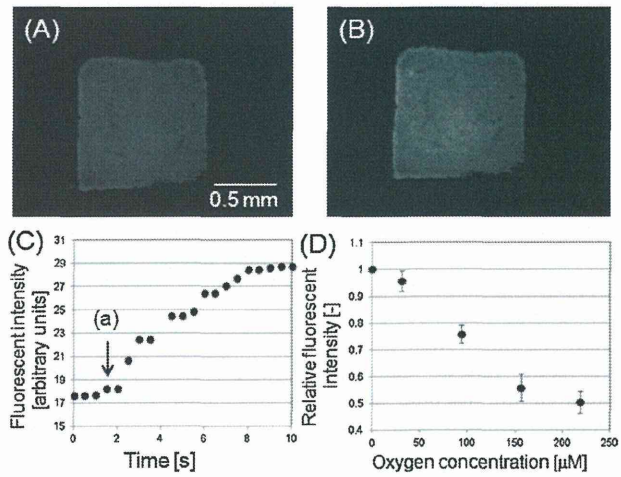

Figure 4. (A, B) Fluorescent images of the oxygen responsive microparticles in PBS(−) at a dissolved oxygen concentration of (A) 185 μM and (B) 0 μM. (C) Typical time-course of the fluorescent intensity change when Na_2SO_3 solution was added into PBS(−) at point (a). (D) Relationship between the relative fluorescent intensity of the imaging sheet and the dissolved oxygen concentration. Oxygen concentration was controlled by gradually adding Na_2SO_3 solution into the previously air-bubbled PBS(−). Each point represents the mean of three measures ± SD.

switched to 2.0 V DC to fix the patterned particles on the bottom ITO surface (Fig. 2B). After flushing out any unattached particles, the 20% (w/v) acrylamide and 1% (w/v) bis-acrylamide monomers including 0.4 vol% ammonium persulfate and 0.1 vol% tetramethylethylenediamine were injected into the channel. The device was left undisturbed for 2 h at room temperature to facilitate gelation (Fig. 2C).[7] The resulting sheet was cut into square (10 mm × 10 mm). The fluorescence of the particles was monitored using a fluorescent microscope (Olympus). The particles were excited at 520–550 nm using a mercury lamp and a bandpass filter, and a broad fluorescence emission was observed at around 650 nm.

2.4 Preparation of GOD-modified microparticle pattern on a glass substrate

Amino-functionalized microparticle suspension (1.0 μm diameter, Micromod) was dropped onto the stencil-attached amino-silanized glass substrate and evaporated overnight. The stencil sheet (100 μm thick) has a cross-formed line pattern (line width: 300 μm) made by a cutting plotter (Graphtech). An 8% glutaraldehyde solution was poured onto the particles for 1 h at room temperature to covalently immobilize the particles on the substrate and to functionalize the residual amines on the particles with glutaraldehyde. After washing away the unreacted glutaraldehyde, 1 mg/mL GOD (Wako Pure Chemicals Co.) suspended in PBS(−) (pH 7.0) was poured onto the particles and reacted at 4°C overnight to covalently immobilize the GOD onto the particles. By peeling off the stencil, the GOD-modified microparticle pattern was left on the substrate. 50 mM D-glucose dissolved in PBS(−) was dropped onto the GOD pattern to previously initiate the glucose oxidation. Then, the oxygen imaging sheet was put on the GOD pattern to obtain fluorescent image of oxygen-consuming activity.

3. Results and Discussion

Figure 3 shows snapshots over time of the microparticle patterning using electrohydrodynamic force. Microparticles were introduced into the microchannel to be monodispersed (Fig. 3A). Upon application of the AC electric field, the particles rapidly moved toward the exposed ITO rectangular pattern (Fig. 3B). As demonstrated by several researchers, the application of a low frequency AC electric field drives the particles to move in a direction transverse to the field (toward the bottom ITO electrode pattern) via electrohydrodynamic fluid flow, and the particles accumulate in a two-dimensional ordered structure near the electrode surface.[8] Then, the power supply was switched to DC voltage to immobilize the negatively-charged polystyrene particles on the electrode during the solution change from water to a polyacrylamide prepolymer. Figure 3C shows a photograph of the polyacrylamide hydrogel sheet embedded with the rectangular-shaped sensor particle pattern. The particle transfer efficiency from the ITO electrode surface to the hydrogel was almost 100%.

Figure 4A shows fluorescent images of the oxygen-responsive particles on the hydrogel immersed in PBS(−) dissolving 185 μM oxygen. Oxygen-responsive dye, PtOEP, encapsulated into the particles is based on the ability of molecular oxygen to quench the dye selectively.[9] Therefore, the fluorescent intensity increases as the oxygen concentration decreases. As expected, when Na_2SO_3

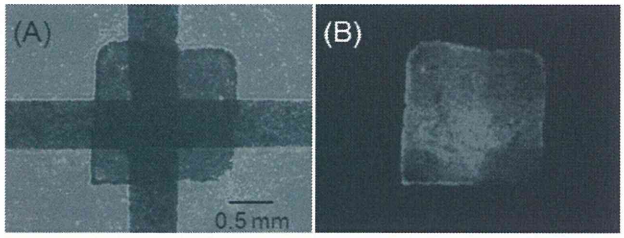

Figure 5. Phase-contrast (A) and fluorescent micrographs (B) of the oxygen imaging sheet attached to the cross-formed GOD-modified microparticles.

(an oxygen scavenger) was added, fluorescent intensity increased (Fig. 4B). 100% response was observed in 6.3 ± 1.2 s after addition of Na_2SO_3 (n = 3, Fig. 4C). Figure 4D shows the inverse relationship between the relative fluorescent intensity of the imaging sheet and the dissolved oxygen concentration measured with a DO meter (Horiba Ltd.). The relative fluorescent intensity indicates the ratio between the fluorescent intensity detected in the absence and the presence of each concentration of oxygen. This result indicated that the gel-sheet can serve as an imaging sensor for dissolved oxygen. The stability of the sensor response was evaluated by measuring the relative fluorescent intensity for PBS(−) every day for a week, showing only 4.2% decrease after 1 week.

Figure 5 demonstrates fluorescent imaging of a GOD-modified microparticle pattern using the oxygen imaging sheet. The imaging sheet was directly attached onto the GOD pattern (Fig. 5A). As can be seen in Fig. 5B, the cross-formed fluorescence displayed corresponds to the GOD pattern. We confirmed there was no response of the imaging sheet against pH change which will be induced by H_2O_2 generation during GOD-catalyzed glucose oxidation. These results suggested that GOD activity was successfully imaged using this patch-type imaging sheet. Non-uniform cross image would be attributed to non-uniform distribution of GOD beads or oxygen sensor beads. Now we are carrying out to optimize electric manipulation of the beads to obtain uniform images.

As mentioned in Introduction, oxygen sensing can be applicable to the study of type 2 diabetes using skeletal muscle cells. Our previous study of scanning electrochemical microscope (SECM) imaging using HeLa cell, which has similar basal respiratory activity with skeletal muscle myoblast,[10] has shown that the difference between the oxygen concentration at the cell surface and the bulk solution far from the cell was ~40 μM.[11] This value corresponds to 0.03 of detectable change in relative fluorescent intensity from the value at bulk oxygen concentration (~200 μM) as estimated from Fig. 4D. The muscle cells enhance their respiratory activities depending on their contractile activities, promising to obtain clear image of contraction-dependent respiratory activity of the cells. During cellular contraction, the sensor beads on the flexible imaging sheet would contract synchronously with the motion of the cells.[12] This characteristic enables continuous monitoring of respiratory activity at same position on the cell surface without concern for disturbance of oxygen concentration gradient around the contracting cells that can cause adverse effect on several oxygen imaging techniques such as SECM.

4. Conclusion

In this study, a patch type oxygen imaging hydrogel sheet was developed. For effective detection of the metabolites in the vicinity of target cells sustaining original hydrogel characteristics, the oxygen sensor beads were locally patterned on the surface of the hydrogel using the electric manipulation technique. We successfully imaged oxygen-consumption activity of GOD pattern as a cellular model, suggesting applicability of the imaging sheet to metabolic bioassays. This flexible sensor sheet is useful for glucose metabolic activity imaging of contracting skeletal muscle cells with supporting cellular contraction to study the relationship between exercise and metabolic activity of muscle in type 2 diabetes.[13]

Acknowledgment

This work was supported by a Core research for Evolutional Science and Technology grant from the Japan Science and Technology Agency.

References

1. M. I. J. Stich, L. H. Fischer, and O. S. Wolfbeis, *Chem. Soc. Rev.*, **39**, 3102 (2010).
2. S. Schreml, R. J. Meier, O. S. Wolfbeis, T. Maisch, R. M. Szeimies, M. Landthaler, J. Regensburger, F. Santarelli, I. Klimant, and P. Babilas, *Exper. Dermat.*, **20**, 550 (2011).
3. S. Schreml, R. J. Meier, O. S. Wolfbeis, M. Landthaler, R. M. Szeimies, and P. Babilas, *Proc. Natl. Acad. Sci. USA*, **108**, 2432 (2011).
4. S. Kimura, K. Matsumoto, K. Mineura, and T. Itoh, *J. Neurol. Sci.*, **258**, 60 (2007).
5. W. Lee, N. J. Cho, A. M. Xiong, J. S. Glenn, and C. W. Frank, *Proc. Natl. Acad. Sci. USA*, **107**, 20709 (2010).
6. X. D. Wang, H. H. Gorris, J. A. Stolwijk, R. J. Meier, D. B. M. Groegel, J. Wegener, and O. S. Wolfbeis, *Chem. Sci.*, **2**, 901 (2011).
7. M. Suzuki, T. Yasukawa, H. Shiku, and T. Matsue, *Langmuir*, **23**, 4088 (2007).
8. K. H. Bhatt, S. Grego, and O. D. Velev, *Langmuir*, **21**, 6603 (2005).
9. K. Montage, K. Komori, F. Yang, T. Tatsuma, T. Fujii, and Y. Sakai, *Photochem. Photobiol. Sci.*, **8**, 1529 (2009).
10. T. C. O'Riordan, A. V. Zhdanov, G. V. Ponomarev, and D. B. Papkovsky, *Anal. Chem.*, **79**, 9414 (2007).
11. M. Nishizawa, K. Takoh, and T. Matsue, *Langmuir*, **18**, 3645 (2002).
12. S. Sekine, Y. Ido, T. Miyake, K. Nagamine, and M. Nishizawa, *J. Am. Chem. Soc.*, **132**, 13174 (2011).
13. K. Nagamine, T. Kawashima, S. Sekine, Y. Ido, M. Kanzaki, and M. Nishizawa, *Lab Chip*, **11**, 513 (2011).